

# Novel efficient process for methanol synthesis by CO<sub>2</sub> hydrogenation

**Citation for published version (APA):**

Kiss, A., Pragt, J. J., Vos, H. J., de Groot, M. T., & Bargeman, G. (2016). Novel efficient process for methanol synthesis by CO<sub>2</sub> hydrogenation. *Chemical Engineering Journal*, 284, 260-269.  
<https://doi.org/10.1016/j.cej.2015.08.101>

**DOI:**

[10.1016/j.cej.2015.08.101](https://doi.org/10.1016/j.cej.2015.08.101)

**Document status and date:**

Published: 01/01/2016

**Document Version:**

Accepted manuscript including changes made at the peer-review stage

**Please check the document version of this publication:**

- A submitted manuscript is the version of the article upon submission and before peer-review. There can be important differences between the submitted version and the official published version of record. People interested in the research are advised to contact the author for the final version of the publication, or visit the DOI to the publisher's website.
- The final author version and the galley proof are versions of the publication after peer review.
- The final published version features the final layout of the paper including the volume, issue and page numbers.

[Link to publication](#)

**General rights**

Copyright and moral rights for the publications made accessible in the public portal are retained by the authors and/or other copyright owners and it is a condition of accessing publications that users recognise and abide by the legal requirements associated with these rights.

- Users may download and print one copy of any publication from the public portal for the purpose of private study or research.
- You may not further distribute the material or use it for any profit-making activity or commercial gain
- You may freely distribute the URL identifying the publication in the public portal.

If the publication is distributed under the terms of Article 25fa of the Dutch Copyright Act, indicated by the "Taverne" license above, please follow below link for the End User Agreement:

[www.tue.nl/taverne](http://www.tue.nl/taverne)

**Take down policy**

If you believe that this document breaches copyright please contact us at:

[openaccess@tue.nl](mailto:openaccess@tue.nl)

providing details and we will investigate your claim.

# 1 **Novel efficient process for methanol synthesis by CO<sub>2</sub> hydrogenation**

2  
3 *Anton A. Kiss,<sup>1,2\*</sup> J. J. Pragt,<sup>1</sup> H. J. Vos,<sup>1</sup> G. Bargeman,<sup>1</sup> M. T. de Groot<sup>3</sup>*

4 <sup>1</sup> *AkzoNobel Research, Development & Innovation, Process Technology SRG, Zutphenseweg*  
5 *10, 7418 AJ Deventer, The Netherlands. E-mail: Tony.Kiss@akzonobel.com*

6 <sup>2</sup> *Sustainable Process Technology Group, Faculty of Science and Technology, University of*  
7 *Twente, PO Box 217, 7500 AE Enschede, The Netherlands*

8 <sup>3</sup> *AkzoNobel, Industrial Chemicals, Competence Team Technology, Stationsstraat 77, 3800*  
9 *AE Amersfoort, The Netherlands*

10 *\* Corresponding author: TonyKiss@gmail.com, Tel: +31 26 366 9420*

## 11 **Keywords**

12 CO<sub>2</sub> hydrogenation, low-pressure process, Cu/Zn catalyst, H<sub>2</sub> stripping, energy efficiency

## 13 **Highlights**

- 14 • Efficient process for methanol synthesis by hydrogenation of carbon dioxide
- 15 • Stripping of products with wet hydrogen for double positive effect
- 16 • Minimum consumption of raw materials, and limited use of electricity and steam

## 17 **Abstract**

18 Methanol is an alternative fuel that offers a convenient solution for efficient energy storage.  
19 Complementary to carbon capture activities, significant effort is devoted to the development  
20 of technologies for methanol synthesis by hydrogenation of carbon dioxide. While CO<sub>2</sub> is  
21 available from plenty of sources, cheap sources of H<sub>2</sub> are less frequently found. An additional  
22 source of hydrogen at industrial scale is the wet hydrogen by-product of chlorine production.  
23 This study is the first to propose an efficient process for methanol synthesis by CO<sub>2</sub> hydro-  
24 genation using wet hydrogen by-product from chlor-alkali production. A key feature of this  
25 novel process is the use of a stripping unit where the wet hydrogen flows in counter-current  
26 mode with the condensed methanol-water mixture resulting from the high-pressure low-  
27 temperature separator after the reaction. This operation has a double positive effect, as it  
28 removes the CO/CO<sub>2</sub> from the methanol-water mixture thus allowing a complete recycle of  
29 CO<sub>2</sub> and avoiding its presence in the product, while also removing the water from the wet  
30 hydrogen thus avoiding the negative impact of adding water on the equilibrium conversion –  
31 with consumption figures of 550 kWh electricity and 0.48-1.16 ton steam per ton methanol.  
32  
33  
34

## 1 **1. Introduction**

2 Methanol is a viable alternative energy source, offering a convenient solution for the efficient  
3 energy storage on a large scale, while playing an important role in economy and sustainability  
4 by converting the CO<sub>2</sub> waste from industry into a valuable product (Olah et al., 2009). At  
5 industrial scale, methanol is produced from synthesis gas (CO/CO<sub>2</sub>/H<sub>2</sub>) using various catalysts  
6 based on CuO/ZnO/Al<sub>2</sub>O<sub>3</sub>. Complementary to carbon capture and sequestration (CCS), much  
7 effort is being put on the development of technologies for methanol production from carbon  
8 dioxide. Several review papers published during the past decade cover this topic very well.  
9 Liu et al. (2003) reviewed the progress in the catalyst innovation, optimization of the reaction  
10 conditions, reaction mechanism, and catalyst performance in CO and CO<sub>2</sub> hydrogenation to  
11 methanol, highlighting the key issues of catalyst improvement and areas of priority in R&D.  
12 Centi and Perathoner (2009) analyzed the possibilities of converting CO<sub>2</sub> to fuels, noting that  
13 the requisites for this objective are: minimization of the consumption of hydrogen (sources),  
14 production of fuels that can be easily stored and transported, and the use of renewable energy  
15 sources. Their review included CO<sub>2</sub> reverse water-gas shift (WGS) and hydrogenation to  
16 hydrocarbons, alcohols, dimethyl ether or formic acid, as well as the reaction to synthesis gas;  
17 photo- and electrochemical/catalytic conversion; and thermo-chemical conversion.  
18 Kondratenko et al. (2013) discussed the heterogeneously catalyzed hydrogenation, as well as  
19 the photocatalytic and electrocatalytic conversion of CO<sub>2</sub> to hydrocarbons or oxygenates,  
20 along with the design of electrodes to improve their performance and the recent developments  
21 of the application of ionic liquids as electrolytes and of microorganisms as co-catalysts.  
22 Saeidi et al. (2014) focused on hydrocarbon and methanol synthesis as methods to convert  
23 CO<sub>2</sub> to value-added products. The reaction mechanisms as well as the effects of catalyst,  
24 reactor type and operating conditions on product efficiency enhancement of each process  
25 were reviewed. Also a brief overview on the reactor types and configurations was provided.  
26 Yan et al. (2014) concentrated on the recent advances in designing efficient catalysts for the  
27 hydrogenation of CO<sub>2</sub> to fuels, e.g. CO<sub>2</sub> hydrogenation to methanol, CO<sub>2</sub> conversion to CO  
28 via reverse WGS reaction and production of hydrocarbons through Fischer-Tropsch synthesis.  
29 Jadhav et al. (2014) tackled various aspects on the CO<sub>2</sub> hydrogenation reaction system such  
30 as: thermodynamics, innovations in catalysts, influences of reaction variables, overall catalyst  
31 performance, reaction mechanism and kinetics, and recent technological advances.  
32 While plenty of CO<sub>2</sub> is available from CCS activities, flue gas or as by-product in various  
33 processes (e.g. bioethanol production), the sources of hydrogen are more limited but feature  
34 processes such as steam methane reforming, coal gasification, partial oxidation of light oil

1 residues, dry reforming, water electrolysis, sulfur-iodine or copper chloride processes (Jadhav  
2 et al., 2014). Another major industrial source is the chlor-alkali process, where H<sub>2</sub> is formed  
3 as by-product of the salt electrolysis. Based on stoichiometry, 1 ton of chlorine leads to 28 kg  
4 hydrogen that can be further converted into 149 kg methanol, using 205 kg CO<sub>2</sub>.

5 This article is the first to propose an efficient process for the CO<sub>2</sub> conversion to methanol  
6 using wet hydrogen (saturated with water) from brine electrolysis, in a catalytic process based  
7 on highly active Cu/Zn/Al/Zr fibrous catalyst (Kiss et al., 2013). For convenience, the results  
8 are provided for a 100 ktpy methanol plant, rigorously simulated in Aspen Plus and including  
9 experimental data previously reported in literature (An et al., 2009).

## 11 **2. Problem statement**

12 Methanol synthesis requires efficient chemical processes and inexpensive raw materials.  
13 Converting carbon dioxide to methanol by hydrogenation is considered to be a great industrial  
14 opportunity (Olah et al., 2009). While cheap CO<sub>2</sub> is available from many sources, the options  
15 for low-cost hydrogen are rather limited. An interesting option is the use of wet hydrogen  
16 available as by-product in the chlor-alkali production. The issue is that the direct use of water  
17 saturated hydrogen stream has a strong negative impact on the chemical equilibrium. To solve  
18 this issue, an efficient process is proposed that includes a key feature – namely the use of  
19 stripper that has a double positive effect as it removes the CO<sub>2</sub> from the methanol-water  
20 mixture produced and avoids the presence of CO/CO<sub>2</sub> in the products, while also removing  
21 the water from the wet hydrogen feed initially saturated with water. The efficiency of the  
22 process is thus increased, leading to low consumption figures.

## 24 **3. Process simulation**

25 This section presents the main results for a plant producing 100 ktpy methanol, by CO<sub>2</sub>  
26 hydrogenation using a highly active Cu/Zn/Al/Zr fibrous catalyst (An et al., 2009).

### 28 **3.1 Property model**

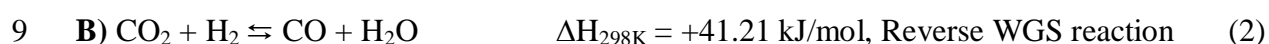
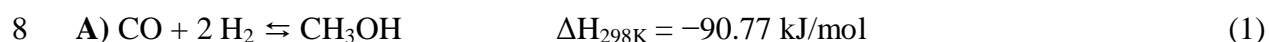
29 The complete process was rigorously simulated in Aspen Plus using the RK-Soave property  
30 model which is most suitable for these components (H<sub>2</sub>, CO, CO<sub>2</sub>, H<sub>2</sub>O, and CH<sub>3</sub>OH) and  
31 conditions (pressure up to 50 bar and temperature up to 250 °C). The non-random two-liquid  
32 (NRTL) model was used complementary to the RK-Soave property model, for modeling the  
33 distillation section operating at low pressure and in which no hydrogen is present. This is in  
34 line with literature recommendations for such systems (Kiss, 2013; Dimian et al., 2014). Note

1 that all the binary interaction parameters related to the property models RK-Soave and NRTL  
2 are available in the pure components databank of the Aspen Plus process simulator.

3

### 4 **3.2 Chemical reactions**

5 The pathways for methanol formation from CO<sub>2</sub>/CO and H<sub>2</sub> on a metallic Cu catalyst are  
6 given in Kondratenko et al. (2013). The actual chemistry of CO<sub>2</sub> hydrogenation involves three  
7 main equilibrium reactions (A, B and C) leading to methanol and water (Fiedler et al., 2005):



11 The CO<sub>2</sub> conversion to CO (reaction B) is endothermic hence the temperature increase is  
12 favorable to the equilibrium. However, the CO and CO<sub>2</sub> conversions to methanol (reactions A  
13 and C) are exothermic hence the temperature increase has a negative impact on equilibrium.  
14 Thus, higher methanol yields are obtained at lower temperatures and higher pressures. This  
15 effect is clearly illustrated in Figure 1 showing the effect of temperature on equilibrium.

16 Note that in a process having all three components (CO<sub>2</sub>, CO, and H<sub>2</sub>) in the feed, the mole  
17 fractions have to be adjusted such that the optimal stoichiometric number (SN) is equal to 2.  
18 A higher value (SN > 2) indicates that there is an excess of H<sub>2</sub> in the feed gas, while a lower  
19 value (SN < 2) means that there is an excess of carbon. When only CO<sub>2</sub> and H<sub>2</sub> are present in  
20 the feed, a H<sub>2</sub>:CO<sub>2</sub> ratio of 3:1 ensures that SN=2. The SN number is calculated as follows:

21 
$$SN = \frac{y_{\text{H}_2} - y_{\text{CO}_2}}{y_{\text{CO}} + y_{\text{CO}_2}}$$
      (4)

22

### 23 **3.3 Chemical equilibrium**

24 The values for the equilibrium constants ( $K_A$ ,  $K_B$  and  $K_C$ ) were reported by Lim et al. (2009),  
25 using  $R=8.314 \text{ J/mol.K}$  and  $K_i$ . Note that the study of Lim et al. (2009) used the experimental  
26 data from Graaf et al. (1986), so basically it is the same data but provided in an explicit model  
27 which provides a consistent framework for process simulations in Aspen Plus.

28 The comparison between the data from literature (Lim et al. 2009) and the equilibrium  
29 constant values evaluated within Aspen Plus using the equilibrium reactor showed an  
30 excellent agreement. Note that in Aspen Plus, the equilibrium constants are evaluated based

1 upon fugacity in [atm]. A conversion was made to [Pa] based correlations as those will be  
2 required to express the driving force term of the kinetic rate equations.

$$3 \quad \ln K_A = \frac{9.8438 \times 10^4}{RT} - 29.07 \rightarrow K_A = 2.3717 \times 10^{-13} \exp\left(\frac{9.8438 \times 10^4}{RT}\right) [\text{atm}^{-2}]$$

$$4 \quad \ln K_A = -52.096 + \frac{11840}{T} \quad \text{with } K_A [\text{Pa}^{-2}] \quad (5)$$

$$5 \quad \ln K_B = \frac{-4.3939 \times 10^4}{RT} + 5.639 \rightarrow K_B = 2.8118 \times 10^2 \exp\left(\frac{-4.3939 \times 10^4}{RT}\right) [-]$$

$$6 \quad \ln K_B = 5.639 + \frac{-5285}{T} \quad \text{with } K_B [-] \quad (6)$$

$$7 \quad K_C = K_A \times K_B \rightarrow K_C = 6.6688 \times 10^{-11} \exp\left(\frac{5.4499 \times 10^4}{RT}\right) [\text{atm}^{-2}]$$

$$8 \quad \ln K_C = -46.457 + \frac{6555}{T} \quad \text{with } K_C [\text{Pa}^{-2}] \quad (7)$$

9

### 10 **3.4 Catalyst and kinetics**

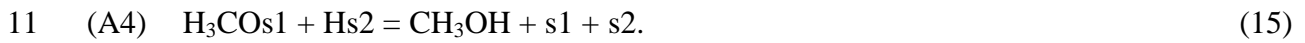
11 Many catalysts are available for CO<sub>2</sub> hydrogenation, based on Cu/Zn formulations (Yan et al.,  
12 2014). Also most of the commercial catalysts available from several catalyst manufacturers  
13 (e.g. Katalko from Johnson-Matthey, MegaMax from Clariant) have high performance. In this  
14 work, the kinetic model A3B2C3 – which was shown to be the best kinetic model out of the  
15 48 models tested by Graaf et al. (1988) – combined with kinetic data from An et al. (2009)  
16 was implemented in Aspen Plus. Note that other adequate kinetic models are also available in  
17 the literature (Bos et al. 1989; Vanden Bussche and Froment 1996; Coteron and Hayhurst,  
18 1994; and numerous publications from Haldor Topsoe).

19 The experimental data from An et al. (2009) validates the model of Graaf et al (1988) and it  
20 was obtained for a fibrous Cu/Zn/Al/Zr catalyst that was designed especially for the  
21 hydrogenation of CO<sub>2</sub>. Note that the Langmuir-Hinshelwood kinetic model assumes two  
22 different active sites. CO and CO<sub>2</sub> adsorb competitively on the so called s1-sites, while H<sub>2</sub>  
23 and H<sub>2</sub>O are adsorbed competitively on the s2-sites. According to Graaf et al. (1988) the  
24 adsorption of methanol is assumed to be negligible, while H<sub>2</sub> is believed to adsorb  
25 dissociatively – hence the use of  $\lambda_H$  term. Nonetheless, it is rather straightforward to derive  
26 alternative kinetic rate expressions that are based on the molecular adsorption of H<sub>2</sub>. The  
27 elementary reactions are described as follows (Graaf et al., 1988):

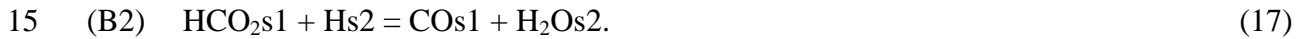
28

1 *Adsorption equilibria*

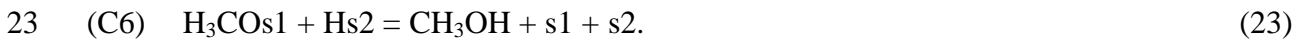
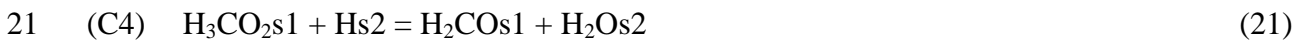
6

7 *Reaction (A)*

12

13 *Reaction (B)*

16

17 *Reaction (C)*

24 In case of the best model concluded by Graaf et al. (1988) the rate controlling steps for each  
 25 overall reaction A, B and C are A3, B2, and C3 respectively – hence the notation A3B2C3.

26

27 The corresponding rate equations for the kinetic model A3B2C3 are:

$$28 \quad r_{CH_3OH,A3} = k_A \frac{K_{CO} \left[ f_{CO} f_{H_2}^{3/2} - f_{CH_3OH} / (K_A \sqrt{f_{H_2}}) \right]}{\left( 1 + K_{CO} f_{CO} + K_{CO_2} f_{CO_2} \right) \left[ \sqrt{f_{H_2}} + (K_{H_2O} / \sqrt{K_H}) f_{H_2O} \right]} \quad (24)$$

$$29 \quad r_{CO,B2} = r_{H_2O,B2} = k_B \frac{K_{CO_2} \left[ f_{CO_2} f_{H_2} - f_{H_2O} f_{CO} / K_B \right]}{\left( 1 + K_{CO} f_{CO} + K_{CO_2} f_{CO_2} \right) \left[ \sqrt{f_{H_2}} + (K_{H_2O} / \sqrt{K_H}) f_{H_2O} \right]} \quad (25)$$

$$1 \quad r_{CH_3OH,C3} = r_{H_2O,C3} = k_C \frac{K_{CO_2} \left[ f_{CO_2} f_{H_2}^{3/2} - f_{H_2O} f_{CH_3OH} / (f_{H_2}^{3/2} K_C) \right]}{\left( 1 + K_{CO} f_{CO} + K_{CO_2} f_{CO_2} \right) \left[ \sqrt{f_{H_2}} + (K_{H_2O} / \sqrt{K_H}) f_{H_2O} \right]} \quad (26)$$

2 For example, the origin of  $r_{CH_3OH,A3}$  is explained hereafter.

$$3 \quad r_{A3+} = k_{A3+} \theta_{H_2CO} \lambda_H \quad (27)$$

$$4 \quad K_{A1} = \frac{\theta_{HCO}}{\theta_{CO}} \cdot \frac{\lambda_e}{\lambda_H} = \frac{\theta_{HCO}}{\theta_{CO}} \cdot \frac{1}{\sqrt{K_H f_{H_2}}} \quad \text{and} \quad K_{A2} = \frac{\theta_{H_2CO}}{\theta_{HCO}} \cdot \frac{\lambda_e}{\lambda_H} = \frac{\theta_{H_2CO}}{\theta_{HCO}} \cdot \frac{1}{\sqrt{K_H f_{H_2}}} \quad (28)$$

5 Therefore:

$$6 \quad \theta_{H_2CO} = K_{A1} K_{A2} \left( \frac{\lambda_H}{\lambda_e} \right)^2 \theta_{CO} = K_{A1} K_{A2} K_H f_{H_2} \theta_{CO} \quad (29)$$

$$7 \quad r_{A3+} = k_{A3+} K_{A1} K_{A2} K_H f_{H_2} \theta_{CO} \lambda_H \quad (30)$$

$$8 \quad r_{A3+} = k_{A3+} K_{A1} K_{A2} \frac{K_{CO} f_{CO} (K_H f_{H_2})^{3/2}}{\left( 1 + K_{CO} f_{CO} + K_{CO_2} f_{CO_2} \right) \left( 1 + \sqrt{K_H f_{H_2}} + K_{H_2O} f_{H_2O} \right)} \quad (31)$$

9 The equilibrium constant of the overall reaction (A) is used to define the driving force term:

$$10 \quad K_A = \frac{f_{CH_3OH}}{f_{CO} f_{H_2}^2} \rightarrow \text{Driving force} = f_{CO} f_{H_2}^{3/2} - f_{CH_3OH} / (K_A \sqrt{f_{H_2}}) \quad (32)$$

11 As a result it follows that:

$$12 \quad r_A = r_{A3+} - r_{A3-} = k_{A3+} K_{A1} K_{A2} \frac{K_{CO} K_H^{3/2} \left( f_{CO} f_{H_2}^{3/2} - f_{CH_3OH} / (K_A \sqrt{f_{H_2}}) \right)}{\left( 1 + K_{CO} f_{CO} + K_{CO_2} f_{CO_2} \right) \left( 1 + \sqrt{K_H f_{H_2}} + K_{H_2O} f_{H_2O} \right)} \quad (33)$$

13 According to Graaf et al. (1988) it holds:

$$14 \quad 1 \ll \sqrt{K_H f_{H_2}} + K_{H_2O} f_{H_2O} \quad (34)$$

15 Thus:

$$16 \quad r_A = k_{A3+} K_{A1} K_{A2} \frac{K_{CO} K_H \left( f_{CO} f_{H_2}^{3/2} - f_{CH_3OH} / (K_A \sqrt{f_{H_2}}) \right)}{\left( 1 + K_{CO} f_{CO} + K_{CO_2} f_{CO_2} \right) \left( \sqrt{f_{H_2}} + (K_{H_2O} / \sqrt{K_H}) f_{H_2O} \right)} \quad (35)$$

17 Comparing this with the result presented by Eq. 43 in Graaf et al. (1988), it is concluded that:

$$18 \quad k_A = k_{A3+} K_{A1} K_{A2} K_H \quad (36)$$

19 The origin of the other terms ( $r_{CO,B2}$  and  $r_{CH_3OH,C3}$ ) can be explained in a similar way.

20 The generalized rate expression to be used in Aspen Plus is given by:

$$21 \quad r = \frac{(\text{kinetic factor})(\text{driving force expression})}{(\text{adsorption term})} \quad (37)$$

22 When a reference temperature  $T_o$  is not specified, the kinetic factor in Aspen is expressed by a



1 pre-exponential factor and an Arrhenius term:  $kinetic\ factor = kT^n \exp(-E_a / RT)$ . All the  
 2 required input data for the kinetic factor are included in Table 1 (An et al., 2009). Note that  
 3 the units for the pre-exponential constant depend on the units of the driving force term and the  
 4 adsorption term. Therefore the units are not the same for all of the reactions.

5 The driving force expressions are as follows:

$$6 \text{ Reaction A: } K_{CO} f_{CO} f_{H_2}^{3/2} - \frac{K_{CO}}{K_A} f_{CH_3OH} f_{H_2}^{-1/2} [Pa^{3/2}] \quad (38)$$

$$7 \text{ Reaction B: } K_{CO_2} f_{CO_2} f_{H_2} - \frac{K_{CO_2}}{K_B} f_{H_2O} f_{CO} [Pa] \quad (39)$$

$$8 \text{ Reaction C: } K_{CO_2} f_{CO_2} f_{H_2}^{3/2} - \frac{K_{CO_2}}{K_C} f_{H_2O} f_{CH_3OH} f_{H_2}^{-3/2} [Pa^{3/2}] \quad (40)$$

9 Note that in Aspen Plus, the driving force is expressed in a generalized form:

$$10 K_1 \left( \prod c_i^{v_i} \right) - K_2 \left( \prod c_j^{v_j} \right) \quad (41)$$

11 When selecting the vapor phase as the reactive phase, and neglecting the difference between  
 12 partial pressure and fugacity (i.e. assuming ideal gas), the partial pressures are used for the  
 13 concentration. The resulting values for  $K_1$  and  $K_2$  are given in Table 2. In Aspen Plus,  $K_1$  and  
 14  $K_2$  are expressed in a logarithmic form, so the resulting input parameters are given in Table 3.

$$15 \ln(K) = A + \frac{B}{T} \quad (42)$$

16 The adsorption term is the same for all reactions. The expression applied in Aspen Plus is:

$$17 \left( \sum K_i \left[ \prod c_j^{v_j} \right] \right)^m \quad (43)$$

18 Configuring Aspen Plus requires re-writing the adsorption term in the kinetic expression,  
 19 which is the same for all three reactions (Graaf et al., 1988):

$$20 \left( 1 + K_{CO} f_{CO} + K_{CO_2} f_{CO_2} \right) \left( f_{H_2}^{1/2} + \left[ K_{H_2O} / \sqrt{K_H} \right] f_{H_2O} \right) [bar^{1/2}] = \quad (44)$$

$$21 \frac{\sqrt{f_{H_2}} + \frac{K_{H_2O}}{\sqrt{K_H}} f_{H_2O} + K_{CO} f_{CO} \sqrt{f_{H_2}} + \frac{K_{CO} K_{H_2O}}{\sqrt{K_H}} f_{CO} f_{H_2O} + K_{CO_2} f_{CO_2} \sqrt{f_{H_2}} + \frac{K_{CO_2} K_{H_2O}}{\sqrt{K_H}} f_{CO_2} f_{H_2O}}{\left( 1 + K_{CO} f_{CO} + K_{CO_2} f_{CO_2} \right) \left( f_{H_2}^{1/2} + \left[ K_{H_2O} / \sqrt{K_H} \right] f_{H_2O} \right)}$$

22 Both the numerator and the denominator of the kinetic rate equation are divided by  $\sqrt{K_H}$  in  
 23 order to reduce the number of variables since this allows lumping together  $K_H$  and  $K_{H_2O}$ .

24 Although the result is that the adsorption term is not dimensionless anymore, the result is  
 25 mathematically the same for the reaction rate expression. This expression is the sum of 6  
 26 terms with the exponent  $m=1$ . The combined  $K_i$  factors for each term are specified in Table 4.

27 The adsorption constants are a function of temperature:

$$K_i = a_i \exp(b_i / RT) \quad (45)$$

Note that in Aspen Plus,  $K$  is expressed in a logarithmic form – for convenience, the resulting input parameters are also provided in Table 4.

$$\ln(K) = A + \frac{B}{T} \quad (46)$$

Finally, the LHHW-kinetics was configured in Aspen Plus and tested with a plug flow reactor (PFR) against equilibrium and kinetics data from literature (An et al., 2009). An excess of catalyst was applied in order to reach the chemical equilibrium in the PFR. The comparison between the experimental and simulated data (illustrated in Table 5) shows a good agreement with less than 5% error around the operating process conditions, thus indicating a correctly implementation of the kinetics. No model parameters were calculated and no changes were made to the kinetic data from An et al. (2009) and the equilibrium data from Lim et al. (2009) – based on the detailed model of Graaf et al. (1986). These were only translated from the implicit form to the explicit input format required by the process simulator Aspen Plus.

14

## 4. Results and discussion

### 4.1.1 Sensitivity analysis

Within Aspen Plus, the CO<sub>2</sub> converter was simulated by a plug-flow reactor (PFR) using the Soave-Redlich-Kwong EOS and NRTL with Henry components as property models. The amount of catalyst considered in the reactor corresponds to a gas hourly space velocity of GHSV=5.9 m<sup>3</sup>/kg<sub>cat</sub>h. Due to the geometrical design of the multi-tubular reactor, the gas velocity does not exceed 1.5 m/s. The following parameters were varied in the specified range:  $T=200-300^\circ\text{C}$ ,  $p=1-100$  bar, reactants ratio  $R=\text{H}_2:\text{CO}_2=3-12$ , and catalyst loadings within the range  $\text{GHSV}=0.1-10^5$  m<sup>3</sup>/kg<sub>cat</sub>h. The following figures show the main results of the sensitivity analysis, in terms of methanol and CO yield as a function of temperature (Figure 2 and Figure 3), pressure (Figure 4) and catalyst loading (Figure 5), at different reactants ratios. Due to the kinetic limitations at lower temperatures versus equilibrium limitations at higher temperatures, an optimal operating region exists and this depends on the reactants ratio. The effect of pressure on the MeOH and CO yields is straightforward. The formation of methanol is clearly favored at higher pressures due to the fact that CO<sub>2</sub> and CO hydrogenation reactions proceed with a decrease of the total number of moles. Consequently, as more CO is converted to methanol at higher pressures, the CO yield decreases when the pressure is increased. Figure 5 shows that at 200°C the reaction is kinetically limited, as an increase in catalyst loading leads to an increase in methanol yield. Therefore, it makes sense to increase the catalytic

1 activity at lower temperatures in order to improve the yield. However, at higher temperatures  
2 (>250°C) the reaction is equilibrium limited when a sufficient amount of catalyst is used  
3 (GHSV<10 m<sup>3</sup>/kg<sub>cat</sub>h), hence any further increase of the catalyst loading has no effect at all.  
4 Furthermore, Figure 6 shows the theoretical effect of water content in the reactor feed – more  
5 water leads to decreased performance as the presence of water has a detrimental effect on the  
6 equilibrium. However, it should be noted that in this new process the humidity (water content)  
7 of the hydrogen feed is not an actual variable, since the fresh feed stream is assumed to be  
8 saturated with water at ambient conditions hence this is the worst case scenario.

#### 10 **4.1.2 Process description**

11 The classic low-pressure methanol process follows the generic scheme shown in Figure 7  
12 (Fiedler et al., 2005) – which is a typical reaction-separation-recycle system (Kiss, 2010; Kiss  
13 et al., 2007). Basically, the reactants are brought to the required temperature and pressure then  
14 fed together (matching the stoichiometric number  $SN=2$ ) to a reactor operated at 200-300°C  
15 and 50-100 bar. Due to the chemical equilibrium limitations, the conversion is incomplete so  
16 the reactor outlet will comprise of products (methanol and water) as well as unconverted  
17 reactants (CO<sub>x</sub> and hydrogen). This gaseous mixture is cooled and flashed to separate the  
18 condensable products from the non-condensable reactants, which are recycled. The condensed  
19 components are then separated in two steps, typically by a direct distillation sequence, into  
20 lights (dissolved CO<sub>x</sub> and minor light impurities), methanol and a water stream.

21 In this work, a plant capacity of 100 ktpy methanol is considered. Figure 8 presents the  
22 proposed process flowsheet, while the complete mass and energy balance is provided in Table  
23 6. Compared to the classic low-pressure methanol process reported (Fiedler et al., 2005) there  
24 are several key differences, described hereafter. The fresh CO<sub>2</sub> feed stream is mixed with the  
25 recycle gas stream and fed to the feed-effluent-heat-exchanger (FEHE) without decompression  
26 and heating. This leads to a lower gas flowrate to the recycle compressor (COMP2) and thus  
27 reduced requirements of electricity.

28 Note that using classic process synthesis heuristics we have also evaluated alternative process  
29 configurations that aimed to take advantage of having separate hydrogen and CO<sub>2</sub> feed  
30 streams (e.g. higher flexibility and methanol yield, lower energy requirements). However, no  
31 significant improvement was observed by feeding the reactants as mixed or pure components  
32 all at once or added along the catalytic reactor. The main reason is that the reactor outlet is in  
33 all cases close to the equilibrium hence implicitly limited. Consequently, the strategy of  
34 feeding the reactants has no effect on a reactor reaching 100% of the equilibrium conversion.

1 The best alternative strategy was to feed the mixed reactants along the reactor working at  
2 lower end temperature, and to strip out the dissolved CO<sub>2</sub> from the methanol using the fresh  
3 feed of hydrogen that is then mixed with the CO<sub>2</sub> and the recycle stream. This strategy leads  
4 to the highest methanol yield and the lowest energy requirements per ton product. As shown  
5 later, this strategy is especially beneficial when wet fresh hydrogen is used, since the addition  
6 of wet fresh hydrogen does not only result in the stripping and recycling of CO<sub>2</sub> and CO from  
7 the produced methanol, but to removal of the water from the fresh hydrogen as well, thus  
8 leading to even bigger improvements in CO<sub>2</sub> conversion per pass and energy reduction.

9 The fresh wet hydrogen feed from chlorine production by salt electrolysis is pressurized to 45  
10 bar in a primary multi-stage compressor (COMP1). The hydrogen compressor (COMP1) was  
11 optimized (e.g. reducing the intermediate cooling temperature to less than 170 °C) to take  
12 advantage of the compression curve, and therefore further reduce the compression duty. The  
13 resulting gas mixture is heated up in a feed-effluent heat-exchanger (FEHE) by the reactor  
14 outlet stream, and then fed to a multi-tubular plug-flow reactor (PFR) operated isothermally at  
15 50 bar and 250°C. The heat of reaction generated in the reactor can be used to generate high  
16 pressure steam. The multi-tubular catalytic reactor has the following characteristics: 12 m  
17 length, 810 tubes of 0.06 m diameter, and a loading of 865 kg catalyst (Cu/Zn/Al/Zr). More  
18 catalyst could be added, but the improvements on the conversion are not significant since the  
19 operation under these conditions is practically equilibrium limited. A bed voidage (defined as  
20 the fraction of the reactor volume not occupied by catalyst) of 0.98 was used in simulations.  
21 This means that the fibrous Cu/Zn/Al/Zr catalyst reported in An et al. (2009) is taken on a  
22 support and that 0.02 volume fraction (based on reactor) of active catalyst material is used.

23 The reactor outlet stream is cooled down in the FEHE unit and an additional COOLER, then  
24 being eventually flashed in a separator (SEP) to split methanol and water (liquid) from the  
25 non-condensable gas components (CO, CO<sub>2</sub> and H<sub>2</sub>) that are recycled. The recycle stream is  
26 then purged (optionally, up to 1.5%) and mixed with the fresh CO<sub>2</sub> feed stream and sent to the  
27 second compressor (COMP2). The liquid stream of the flash is sent to a stripping column  
28 (STRIPPER) where the compressed wet hydrogen stream from COMP1 is fed in counter-current  
29 mode. This has a double positive effect, as it dries the hydrogen feed thus removing water  
30 from the reactor feed, and it removes the light ends (mainly CO<sub>2</sub> but CO as well) which are  
31 completely recycled thus significantly improving the consumption figures. The liquid bottom  
32 stream of the stripper is sent to a distillation column (DC) that separates water as bottom  
33 product and methanol as high purity top distillate. It is worth noting that by using the stripper  
34 unit, the liquid outlet (containing methanol-water) is obtained at higher temperature – the

1 consequence of using a warmer feed stream to the DC unit being a reduced reboiler duty. Note  
2 that the separation of the methanol-water stream is carried out in a single distillation column  
3 using a partial condenser – able to deliver a vapor distillate (lights), high purity liquid  
4 distillate (methanol) and bottom product (water). Consequently, one distillation column  
5 (including reboiler and condenser) of the conventional direct sequence is spared. A dividing-  
6 wall column can be also considered as an alternative for this ternary separation (Kiss, 2013),  
7 in order to further reduce the (minor) methanol loss in the lights stream.

### 9 **4.1.3 Consumption figures**

10 For convenience, Table 7 gives the key parameters and consumption figures for this process.  
11 Remarkable, a large part of the total reboiler duty (about 60%) can be covered by the thermal  
12 energy produced in the reactor, by generating high pressure steam usable in the reboiler. It is  
13 also worth noting that the consumption of raw materials is extremely close to the minimum  
14 stoichiometric value, while the use of utilities (steam and electricity) is also very low. The  
15 patent of Kiss et al. (2013) includes several comparative examples showing that at various  
16 operating conditions this novel process using hydrogen stripping of products allows 15-20%  
17 energy savings and 5-8% more methanol product as compared to the conventional process.  
18 For convenience, Table 8 shows a comparison between two cases not limited by equilibrium  
19 (without and with stripper) as described in the patent of Kiss et al. (2013) which provide more  
20 details about these cases and covers more possible process configurations. The advantages of  
21 using a stripping unit are clearly illustrated by the lower consumption figures, higher resource  
22 efficiency, as well as higher conversion of the raw materials.

## 24 **5. Conclusions**

25 The methanol synthesis by carbon dioxide hydrogenation is feasible in the new efficient  
26 process proposed here. A key feature of this novel process is the use of a stripping unit where  
27 the wet hydrogen (saturated with water) flows in counter-current with the condensed mixture  
28 methanol-water resulting from the flash separation after reaction. This operation has a double  
29 positive effect, as it removes CO<sub>x</sub> from the methanol-water mixture thus allowing a complete  
30 recycle of CO<sub>2</sub>, while also removing the water from the wet hydrogen (initially saturated with  
31 water) thus avoiding the negative impact on the reaction equilibrium conversion.

32 As a result, the consumption figures indicate a limited use of utilities (550 kWh/ton methanol,  
33 and 0.48-1.16 ton steam per ton methanol) while the use of the raw materials is minimal, as  
34 both reactants are recovered and recycled hence completely converted in the overall process –

1 being limited by the stoichiometry only. While all the carbon from the CO<sub>2</sub> feed ends up in  
 2 the methanol product, the hydrogen valorization is less efficient since only two thirds of  
 3 hydrogen is converted to methanol product, the rest being converted to the water by-product.

4

5 **Notation**6  $A$  pre-exponential factor7  $c$  concentration (mol/kg)8  $f$  fugacity (bar)9  $GHSV$  gas hourly space velocity (m<sup>3</sup>/kg<sub>cat</sub>h)10  $k$  reaction rate constant11  $K_R$  equilibrium constant of reaction  $R$ 12  $K_i$  adsorption constant of component  $i$  (1/bar)13  $m$  number of parameters (-)14  $p$  pressure (bar)15  $R$  gas constant = 8.314 (J/molK)16  $W$  weight of catalyst (kg)17  $y_i$  gas mol fraction of component  $i$  (-)

18

## 19 Greek symbols

20  $\Delta H$  enthalpy change (kJ/mol)21  $\Delta S$  entropy change (kJ/molK)22  $\theta_{CO}$  Langmuir adsorption term CO23  $\theta_{CO_2}$  Langmuir adsorption term CO<sub>2</sub>24  $\theta_i$  fractional occupation of s1-sites with species  $i$ 25  $\lambda_j$  fractional occupation of s2-sites with species  $j$ 26  $\lambda_H$  Langmuir adsorption term for dissociated hydrogen

27

## 28 Subscripts

29  $i$  component  $i$  (e.g. CO, CO<sub>2</sub>, H<sub>2</sub>, CH<sub>3</sub>OH, H<sub>2</sub>O)

30

## 31 Abbreviations

32  $SN$  Stoichiometric number33  $WGS$  Water-gas shift reaction

1  
2  
3  
4  
5  
6  
7  
8  
9  
10  
11  
12  
13  
14  
15  
16  
17  
18  
19  
20  
21  
22  
23  
24  
25  
26  
27  
28  
29  
30  
31  
32  
33  
34

## References

1. Ali K.A., Abdullah A.Z., Mohamed A.R., Recent development in catalytic technologies for methanol synthesis from renewable sources: A critical review, *Renewable and Sustainable Energy Reviews*, 44 (2015), 505-518.
2. An X., Zuo Y., Zhang Q., Wang J., Methanol synthesis from CO<sub>2</sub> hydrogenation with a Cu/Zn/Al/Zr fibrous catalyst, *Chinese Journal of Chemical Engineering*, 17 (2009), 88-94.
3. Bos A.N.R., Borman P.C., Kuczynski M., Westerterp K.R., The kinetics of the methanol synthesis on a copper catalyst: An experimental study, *Chemical Engineering Science*, 44 (1989), 2435-2449.
4. Centi G., Perathoner S., Opportunities and prospects in the chemical recycling of carbon dioxide to fuels, *Catalysis Today*, 148 (2009), 191-205.
5. Coteron A., Hayhurst A.N., Kinetics of the synthesis of methanol from CO + H<sub>2</sub> and CO + CO<sub>2</sub> + H<sub>2</sub> over copper-based amorphous catalysts, *Chemical Engineering Science*, 49 (1994), 209-221.
6. Dimian A.C., Bildea C.S., Kiss A.A., *Integrated design and simulation of chemical processes*, 2nd edition, Elsevier, Amsterdam, 2014.
7. Fiedler E., Grossmann G., Kersebohm D. B., Weiss G., Witte C., Methanol, in *Ullmann's Encyclopedia of Industrial Chemistry*, Wiley-VCH, 2005.
8. Graaf G.H., Sijtsema P.J.J.M., Stamhuis E.J., Joosten G.E.H., Chemical equilibria in methanol synthesis, *Chemical Engineering Science*, 41 (1986), 2883-2890.
9. Graaf G.H., Stamhuis E.J., Beenackers A.A.C.M., Kinetics of low-pressure methanol synthesis, *Chemical Engineering Science*, 43 (1988), 3185-3195.
10. Jadhav S.G., Vaidya P.D., Bhanage B.M., Joshi J.B., Catalytic carbon dioxide hydrogenation to methanol: A review of recent studies, *Chemical Engineering Research and Design*, 92 (2014), 2557-2567.
11. Kiss A.A., *Process design and control by nonlinear analysis: Applications to reactor-separator-recycle systems*, Lambert Academic Publishing, Cologne, Germany, 2010.
12. Kiss A.A., *Advanced distillation technologies - Design, control and applications*. Wiley, Chichester, UK, 2013.
13. Kiss A.A., Bildea C.S., Dimian A.C., Design and control of recycle systems by non-linear analysis, *Computers & Chemical Engineering*, 31 (2007), 601-611.
14. Kiss A.A., Pragt J.J., van Iersel M.M., Bargeman G., de Groot M.T., Continuous process for the preparation of methanol by hydrogenation of carbon dioxide, Patent No.

- 1 WO/2013/144041 (EP-2831025), 2013.
- 2 15. Kondratenko E.V., Mul G., Baltrusaitis J., Larrazábal G.O., Pérez-Ramírez J., Status and  
3 perspectives of CO<sub>2</sub> conversion into fuels and chemicals by catalytic, photocatalytic and  
4 electrocatalytic processes, *Energy and Environmental Science*, 6 (2013), 3112-3135.
- 5 16. Lim H.W., Park M.J., Kang S.H., Chae H.J., Bae J.W, Jun K.W., Modeling of the kinetics  
6 for methanol synthesis using Cu/ZnO/Al<sub>2</sub>O<sub>3</sub>/ZrO<sub>2</sub> catalyst: Influence of carbon dioxide  
7 during hydrogenation, *Industrial & Engineering Chemistry Research*, 48 (2009), 10448-  
8 10455.
- 9 17. Liu X.-M., Lu G.Q., Yan Z.-F., Beltramini J., Recent advances in catalysts for methanol  
10 synthesis via hydrogenation of CO and CO<sub>2</sub>, *Industrial & Engineering Chemistry*  
11 *Research*, 42 (2003), 6518-6530.
- 12 18. Olah G.A., Goepfert A., Surya Prakash G. K., Beyond oil and gas - The methanol  
13 economy, 2nd edition, Wiley-VCH, Weinheim, Germany, 2009.
- 14 19. Saeidi S., Amin N. A. S., Rahimpour M. R., Hydrogenation of CO<sub>2</sub> to value-added  
15 products - A review and potential future developments, *Journal of CO<sub>2</sub> Utilization*, 5  
16 (2014), 66-81.
- 17 20. Vanden Bussche K.M., Froment G.F., A steady-state kinetic model for methanol synthesis  
18 and the water gas shift reaction on a commercial Cu/ZnO/Al<sub>2</sub>O<sub>3</sub> catalyst, *Journal of*  
19 *Catalysis*, 161 (1996), 1-10.
- 20 21. Yan X., Guo H., Yang D., Qiu S., Yao X., Catalytic hydrogenation of carbon dioxide to  
21 fuels, *Current Organic Chemistry*, 18 (2014), 1335-1345.



1 **Tables**

2

3 **Table 1.** Kinetic factor for reactions A, B and C (based on data from An et al., 2009) – the  
 4 units used are [Pa] for fugacity and [mol/g<sub>catalyst</sub>.s] = [kmol/kg<sub>catalyst</sub>.s] for reaction rate

Reaction	k	n	E <sub>a</sub> [J/mol.K]
A	$4.0638 \cdot 10^{-6}$ [kmol./kg <sub>cat</sub> .s.Pa]	0	11695
B	$9.0421 \cdot 10^8$ [kmol./kg <sub>cat</sub> .s.Pa <sup>1/2</sup> ]	0	112860
C	$1.5188 \cdot 10^{-33}$ [kmol./kg <sub>cat</sub> .s.Pa]	0	266010

5

6

7

8

9 **Table 2.** Constants for driving force (adsorption data from An et al., 2009; and chemical  
 10 equilibrium data from Lim et al., 2009).

Reaction	Expression K <sub>1</sub>	K <sub>1</sub>	Expression K <sub>2</sub>	K <sub>2</sub>
A	K <sub>CO</sub> [Pa <sup>-1</sup> ]	$8.3965 \cdot 10^{-11} \exp(118270/RT)$	K <sub>CO</sub> /K <sub>A</sub> [Pa]	$3.5408 \cdot 10^{12} \exp(19832/RT)$
B	K <sub>CO2</sub> [Pa <sup>-1</sup> ]	$1.7214 \cdot 10^{-10} \exp(81287/RT)$	K <sub>CO2</sub> /K <sub>B</sub> [Pa <sup>-1</sup> ]	$6.1221 \cdot 10^{-13} \exp(125226/RT)$
C	K <sub>CO2</sub> [Pa <sup>-1</sup> ]	$1.7214 \cdot 10^{-10} \exp(81287/RT)$	K <sub>CO2</sub> /K <sub>C</sub> [Pa]	$2.5813 \cdot 10^{10} \exp(26788/RT)$

11

12

13

14

15

16 **Table 3.** Constants for driving force (from An et al., 2009) using the format for Aspen Plus

Reaction	K <sub>1</sub>		K <sub>2</sub>	
	A	B	A	B
A	-23.20	14225	28.895	2385
B	-22.48	9777	-28.12	15062
C	-22.48	9777	23.974	3222

17

18

1  
2  
3  
4  
5  
6  
7  
8  
9  
10

**Table 4.**  $K_i$  factors for adsorption term (terms 2, 3, 5 from An et al., 2009; rest is explicitly derived by calculation)

Term	Expression	$a_i$	$b_i$	$\prod c_j^{v_j}$
1	1	$a_1=1$	$b_1=0$	$\sqrt{f_{H_2}}$
2	$\frac{K_{H_2O}}{\sqrt{K_H}}$	$a_2=4.3676 \cdot 10^{-12}$	$b_2=1.1508 \cdot 10^5$	$f_{H_2O}$
3	$K_{CO}$	$a_3=8.3965 \cdot 10^{-11}$	$b_3=1.1827 \cdot 10^5$	$f_{CO} \sqrt{f_{H_2}}$
4	$\frac{K_{CO} K_{H_2O}}{\sqrt{K_H}}$	$a_4=a_2 \cdot a_3$ $a_4=3.6673 \cdot 10^{-22}$	$b_4=b_2+b_3=2.3335 \cdot 10^5$	$f_{CO} f_{H_2O}$
5	$K_{CO_2}$	$a_5=1.7214 \cdot 10^{-10}$	$b_5=8.1287 \cdot 10^4$	$f_{CO_2} \sqrt{f_{H_2}}$
6	$\frac{K_{CO_2} K_{H_2O}}{\sqrt{K_H}}$	$a_6=a_2 \cdot a_5$ $a_6=7.5184 \cdot 10^{-22}$	$b_6=b_2+b_5=1.9727 \cdot 10^5$	$f_{CO_2} f_{H_2O}$

Term	Expression	$A_i=\ln(a_i)$	$B_i=b_i/R$	$\prod c_j^{v_j}$
1	1	0	0	$\sqrt{f_{H_2}}$
2	$\frac{K_{H_2O}}{\sqrt{K_H}}$	-26.1568	13842	$f_{H_2O}$
3	$K_{CO}$	-23.2006	14225	$f_{CO} \sqrt{f_{H_2}}$
4	$\frac{K_{CO} K_{H_2O}}{\sqrt{K_H}}$	-49.3574	28067	$f_{CO} f_{H_2O}$
5	$K_{CO_2}$	-22.4827	9777	$f_{CO_2} \sqrt{f_{H_2}}$
6	$\frac{K_{CO_2} K_{H_2O}}{\sqrt{K_H}}$	-48.6395	23619	$f_{CO_2} f_{H_2O}$

**Table 5.** Comparison of experimental data from An et al. (2009) with the results of the Aspen Plus calculations using LHHW kinetics

<b>SV=6000</b>		<b>CO<sub>2</sub> conversion</b>		<b>Methanol yield based on CO<sub>2</sub> feed</b>	
<b><i>ml/g<sub>cat</sub>.h</i></b>					
<i>T [K]</i>	<i>Experimental data<sup>1</sup></i>	<i>Aspen Plus calculations</i>	<i>Experimental data<sup>1</sup></i>	<i>Aspen Plus calculations</i>	
483	0.170	0.1244	0.110	0.1152	
503	0.225	0.1957	0.155	0.1597	
523	0.255	0.2398	0.178	0.1530	
543	0.250	0.2404	0.140	0.1058	

<b>T=523 K</b>		<b>CO<sub>2</sub> conversion</b>		<b>Methanol yield based on CO<sub>2</sub> feed</b>	
<b><i>SV [ml/g<sub>cat</sub>.h]</i></b>					
	<i>Experimental data<sup>2</sup></i>	<i>Aspen Plus calculations</i>	<i>Experimental data<sup>2</sup></i>	<i>Aspen Plus calculations</i>	
1000	0.262	0.2428	0.193	0.1548	
2000	0.260	0.2428	0.191	0.1548	
4000	0.256	0.2421	0.180	0.1544	
6000	0.250	0.2398	0.166	0.1530	
8000	0.243	0.2362	0.153	0.1509	
10000	0.230	0.2321	0.134	0.1485	

<sup>1</sup> Experimental data taken from Figure 2 reported in An et al. (2009)

<sup>2</sup> Experimental data taken from Figure 4 reported in An et al. (2009)

1 **Table 6.** Mass and energy balance of the proposed process for methanol synthesis

	F-2	F-3	F-3H	F-4	F-5	F-6T	F-7	F-8	F-8STRIP	F-9	F-CO2
Temperature C	42.1	28.2	225.0	93.9	31.0	30.0	30.0	30.0	92.2	87.6	20.0
Pressure bar	50	50	50	50	50	45	45	45	45.2	5.066	100
Vapor Frac	1	0.999	1	0.956	0.900	1	1	0	0	0.001	0
Mole Flow kmol/hr	8649.99	9041.05	9041.05	8259.03	8259.03	8650.00	8649.99	819.06	799.03	799.03	391.06
Mass Flow kg/hr	104793.54	122002.69	122002.69	122002.69	122002.69	104793.65	104793.54	21104.88	19867.90	19867.90	17209.15
Volume Flow cum/hr	4608.29	4572.55	7644.01	4878.20	3822.70	4907.32	4907.32	24.62	25.79	31.68	22.05
Enthalpy Gcal/hr	-185.29	-223.12	-208.89	-226.94	-235.48	-186.07	-186.07	-52.50	-49.30	-49.30	-37.83
Mass Flow kg/hr											
CO	7492.57	7492.57	7492.57	7492.57	7492.57	7492.57	7492.57	2.11	0.00	0.00	0.00
CO2	82810.65	100018.93	100018.93	82810.73	82810.73	82810.73	82810.65	1344.24	0.00	0.00	17208.28
H2	13011.73	13011.73	13011.73	10647.05	10647.05	13011.74	13011.73	1.30	1.45	1.45	0.00
H2O	3.94	4.80	4.80	7048.93	7048.93	3.94	3.94	7045.40	7337.72	7337.72	0.86
CH3OH	1474.66	1474.66	1474.66	14003.40	14003.40	1474.66	1474.66	12711.83	12528.74	12528.74	0.00
Mass Frac CO	0.0715	0.0614	0.0614	0.0614	0.0614	0.0715	0.0715	0.0001	0.0000	0.0000	0.0000
Mass Frac CO2	0.7902	0.8198	0.8198	0.6788	0.6788	0.7902	0.7902	0.0637	0.0000	0.0000	1.0000
Mass Frac H2	0.1242	0.1067	0.1067	0.0873	0.0873	0.1242	0.1242	0.0001	0.0001	0.0001	0.0000
Mass Frac H2O	0.0000	0.0000	0.0000	0.0578	0.0578	0.0000	0.0000	0.3338	0.3693	0.3693	0.0001
Mass Frac CH3OH	0.0141	0.0121	0.0121	0.1148	0.1148	0.0141	0.0141	0.6023	0.6306	0.6306	0.0000
Mole Frac CO	0.0309	0.0296	0.0296	0.0324	0.0324	0.0309	0.0309	0.0001	0.0000	0.0000	0.0000
Mole Frac CO2	0.2175	0.2514	0.2514	0.2278	0.2278	0.2175	0.2175	0.0373	0.0000	0.0000	0.9999
Mole Frac H2	0.7462	0.7139	0.7139	0.6395	0.6395	0.7462	0.7462	0.0008	0.0009	0.0009	0.0000
Mole Frac H2O	0.0000	0.0000	0.0000	0.0474	0.0474	0.0000	0.0000	0.4775	0.5097	0.5097	0.0001
Mole Frac CH3OH	0.0053	0.0051	0.0051	0.0529	0.0529	0.0053	0.0053	0.4844	0.4894	0.4894	0.0000

2

	F-H2	H2-HP	H2-STRIP	HEAVIES	LIGHTS	LIQ	MEOH	PURGE	RX-IN	RX-OUT	VAP
Temperature C	35.0	170.0	47.0	104.9	39.0	30.0	39.0	30.0	225.0	250.0	30.0
Pressure bar	1.1	45	45	1.1	1.013	45	1.013	45	50	50	45
Vapor Frac	1	1	1	0	1	0	0	1	1	1	1
Mole Flow kmol/hr	1190.00	1190.00	1213.51	407.56	1.04	3.48	390.43	0.01	9041.05	8259.03	1210.03
Mass Flow kg/hr	2658.87	2658.87	3985.80	7346.68	12.52	89.96	12508.71	0.10	122002.69	122002.69	3895.84
Volume Flow cum/hr	27734.24	992.69	735.89	8.05	26.70	0.11	16.12	0.00	7644.01	7304.78	695.46
Enthalpy Gcal/hr	-0.86	0.28	-3.13	-27.45	-0.02	-0.22	-22.11	0.00	-208.89	-212.71	-3.10
Mass Flow kg/hr											
CO	0.00	0.00	2.11	0.00	0.00	0.00	0.00	0.01	7492.57	7492.57	2.11
CO2	0.00	0.00	1344.95	0.00	0.00	0.71	0.00	0.08	100018.93	82810.73	1344.24
H2	2366.14	2366.14	2365.99	0.00	1.40	0.01	0.05	0.01	13011.73	10647.05	2365.99
H2O	292.73	292.73	28.08	7336.52	0.00	27.66	1.20	0.00	4.80	7048.93	0.41
CH3OH	0.00	0.00	244.67	10.16	11.12	61.58	12507.46	0.00	1474.66	14003.40	183.09
Mass Frac CO	0.0000	0.0000	0.0005	0.0000	0.0000	0.0000	0.0000	0.0715	0.0614	0.0614	0.0005
Mass Frac CO2	0.0000	0.0000	0.3374	0.0000	0.0000	0.0079	0.0000	0.7902	0.8198	0.6788	0.3450
Mass Frac H2	0.8899	0.8899	0.5936	0.0000	0.1119	0.0001	0.0000	0.1242	0.1067	0.0873	0.6073
Mass Frac H2O	0.1101	0.1101	0.0070	0.9986	0.0000	0.3075	0.0001	0.0000	0.0000	0.0578	0.0001
Mass Frac CH3OH	0.0000	0.0000	0.0614	0.0014	0.8880	0.6846	0.9999	0.0141	0.0121	0.1148	0.0470
Mole Frac CO	0.0000	0.0000	0.0001	0.0000	0.0000	0.0000	0.0000	0.0309	0.0296	0.0324	0.0001
Mole Frac CO2	0.0000	0.0000	0.0252	0.0000	0.0000	0.0046	0.0000	0.2175	0.2514	0.2278	0.0252
Mole Frac H2	0.9863	0.9863	0.9672	0.0000	0.6671	0.0009	0.0001	0.7462	0.7139	0.6395	0.9700
Mole Frac H2O	0.0137	0.0137	0.0013	0.9992	0.0000	0.4416	0.0002	0.0000	0.0000	0.0474	0.0000
Mole Frac CH3OH	0.0000	0.0000	0.0063	0.0008	0.3329	0.5528	0.9998	0.0053	0.0051	0.0529	0.0047

3

1  
2 **Table 7.** Key performance indicators and consumption figures for the proposed process for  
3 methanol synthesis by CO<sub>2</sub> hydrogenation

Parameter	Value	Unit
MeOH production rate	100.07	kton/year
Purge to feed ratio	0	mol/mol
Recycle to feed ratio	5.47	mol/mol
H <sub>2</sub> : CO <sub>2</sub> ratio (feed / reactor inlet)	3.0 / 2.84	mol/mol
H <sub>2</sub> conversion in reactor (per pass)	18.17	%
CO <sub>2</sub> conversion (per pass)	17.20	%
MeOH yield (overall process)	99.83	%
Power of H <sub>2</sub> feed compressor (COMP1)	5962.96	kW
Power of recycle compressor (COMP2)	911.96	kW
Heat generated in the reactor	-4448.72	kW
Heat duty of reboiler (distillation column)	7618.42	kW
Electricity usage (per ton methanol)	550	kWh/ton MeOH
Steam usage (per ton methanol) – no heat integration	1.16	ton steam / ton MeOH
Steam usage (per ton methanol) – heat integrated*	0.48	ton steam / ton MeOH
Electricity cost (at 0.08 €/kWh)	49.37	Euro/ton MeOH
Steam cost (at 25 €/ton steam) – no heat integration	29.03	Euro/ton MeOH
Steam cost (at 25 €/ton steam) – heat integrated*	12.08	Euro/ton MeOH
Pure CO <sub>2</sub> use (per unit of methanol product)	1.3758	kg/kg
Pure H <sub>2</sub> use (per unit of methanol product)	0.1892	kg/kg
Wet H <sub>2</sub> use (per unit of methanol product)	0.2126	kg/kg

4  
5 \* NOTE: The heat integrated option means that part of the steam required in the reboiler of the  
6 distillation column is produced by using the heat generated in the reactor.

7  
8  
9  
10  
11

1  
2 **Table 8.** Comparison of key performance indicators for two cases (without and with stripper)  
3 – as described in the patent of Kiss et al. (2013)

<b>Key performance indicators</b>	<b>Case A-</b>	<b>Case A+</b>	<b>Case B-</b>	<b>Case B+</b>
CO <sub>2</sub> conversion per pass (%)	20.90	21.51	21.50	21.55
CO <sub>2</sub> conversion overall (%)	95.18	99.78	95.18	99.78
Electricity usage (kW.h/ton MeOH)	607	588	597	581
Steam usage (ton steam/ton MeOH) – no HI	1.92	1.52	1.77	1.52
CO <sub>2</sub> use per unit of methanol product (kg/kg)	1.494	1.376	1.443	1.376
H <sub>2</sub> usage per unit of methanol product (kg/kg)	0.197	0.189	0.190	0.189

4  
5 \* NOTE: Case A: Wet hydrogen feed. Case B: Dry hydrogen feed. Both cases are considered  
6 without (–) or with (+) stripper. Operating conditions: P=50 bar, T=225 °C, H<sub>2</sub>:CO<sub>x</sub>=6:1.

7  
8  
9

1 **Figure captions**

2

3 **Figure 1.** Effect of temperature on the equilibrium constants of the main chemical reactions

4

5 **Figure 2.** Effect of temperature on the MeOH and CO yield, at fixed pressure and various  
6 reactants ratios (simulated results)

7

8 **Figure 3.** Effect of temperature on the MeOH and CO yield, at fixed reactants ratio and  
9 various pressures (simulated results)

10

11 **Figure 4.** Effect of pressure on the MeOH and CO yield, at fixed temperature and various  
12 reactants ratios (simulated results)

13

14 **Figure 5.** Effect of the catalyst loading on the MeOH and CO yield (simulated results), at  
15 various reactants ratios and fixed pressure and temperature (p=50 bar, T=200 and T=250 °C)

16

17 **Figure 7.** Generic processing scheme for methanol synthesis from syngas or by CO<sub>2</sub>  
18 hydrogenation

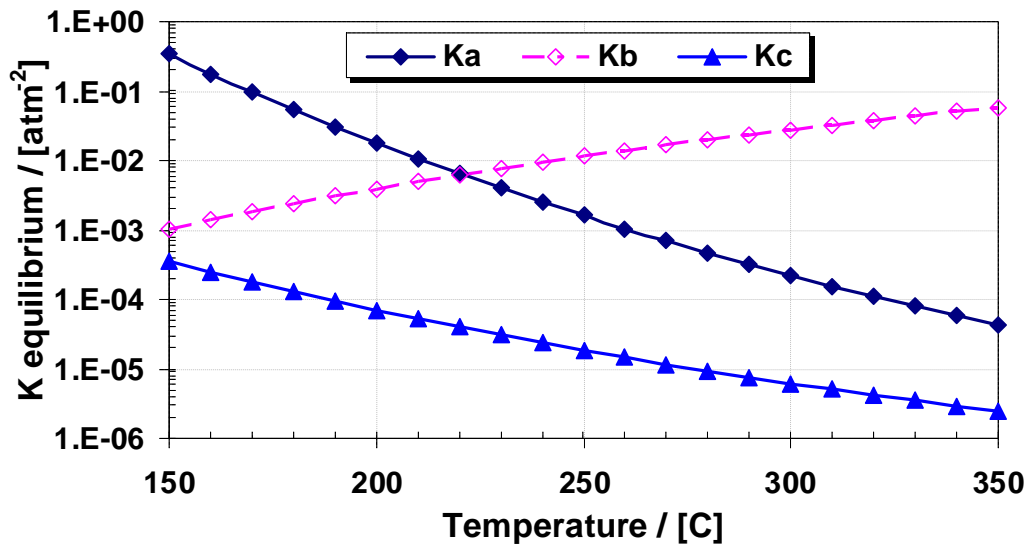
19

20 **Figure 8.** Aspen Plus flowsheet of an efficient process for methanol synthesis by CO<sub>2</sub>  
21 hydrogenation

22

23

1



2

3

Figure 1. Effect of temperature on the equilibrium constants of the main chemical reactions

4

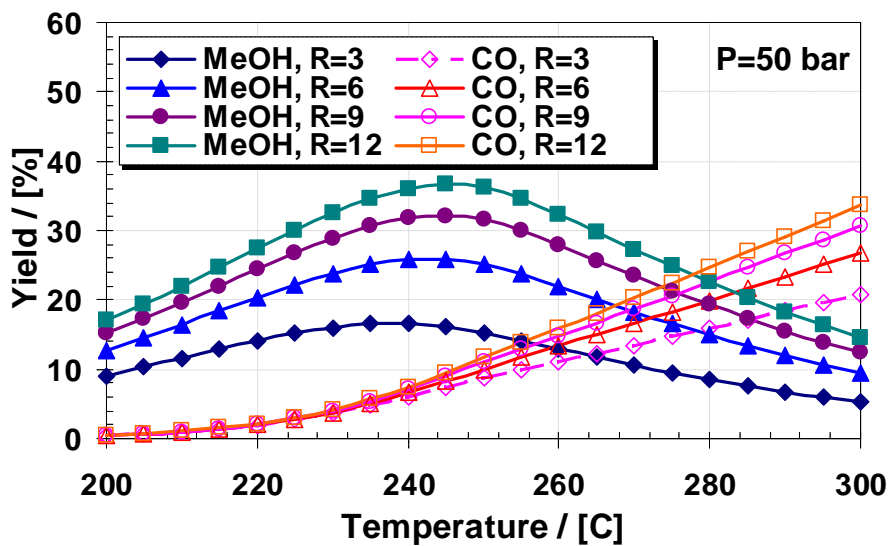
5

6

7

8

9



10

11

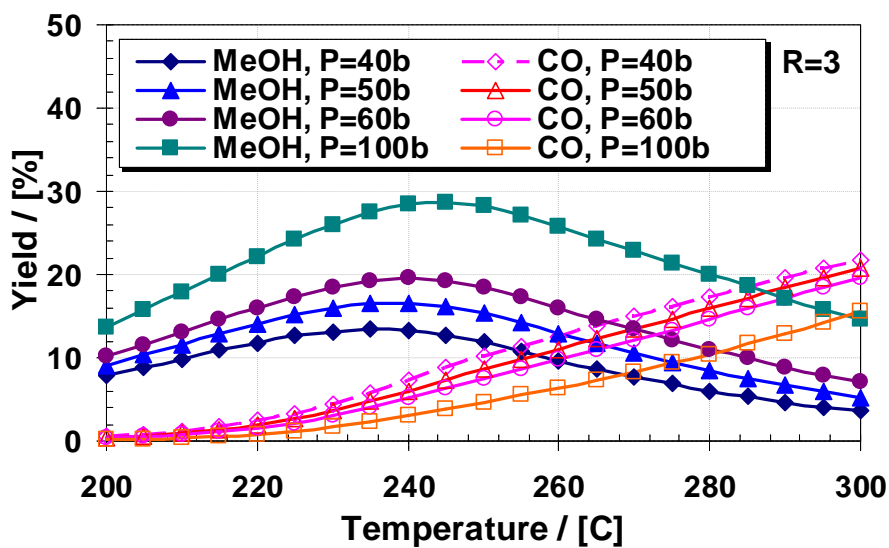
Figure 2. Effect of temperature on the MeOH and CO yield, at fixed pressure and various reactants ratios (simulated results)

12

13



1



2

3

**Figure 3.** Effect of temperature on the MeOH and CO yield, at fixed reactants ratio and various pressures (simulated results)

4

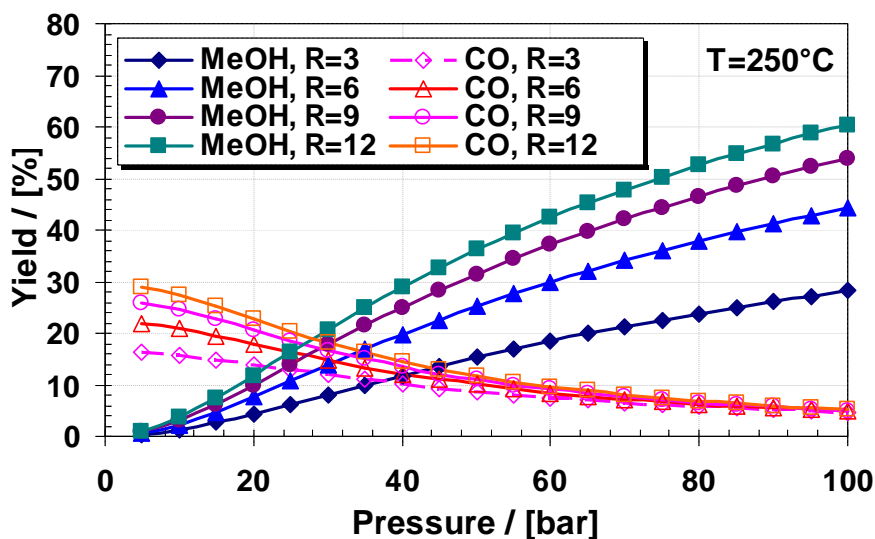
5

6

7

8

9

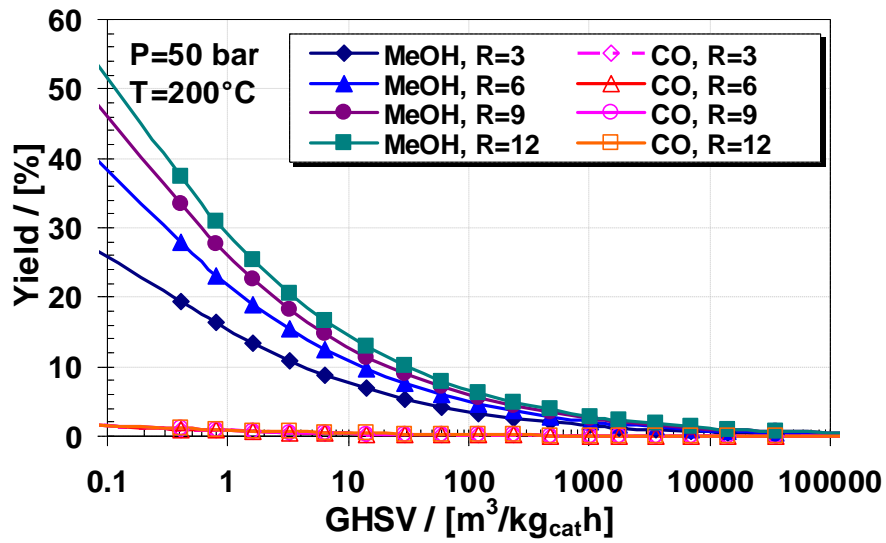


10

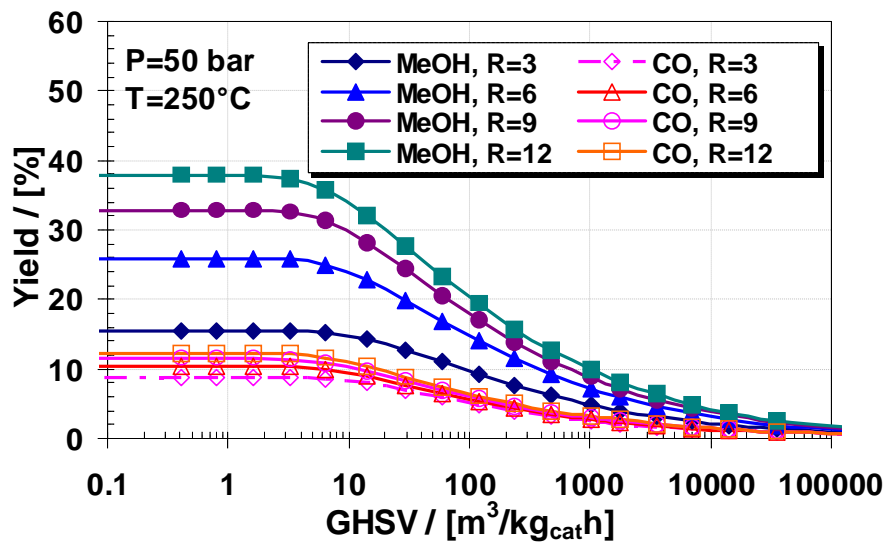
11

**Figure 4.** Effect of pressure on the MeOH and CO yield, at fixed temperature and various reactants ratios (simulated results)

12



1



2

3 **Figure 5.** Effect of the catalyst loading on the MeOH and CO yield (simulated results), at  
 4 various reactants ratios and fixed pressure and temperature (p=50 bar, T=200 and T=250 °C)

5

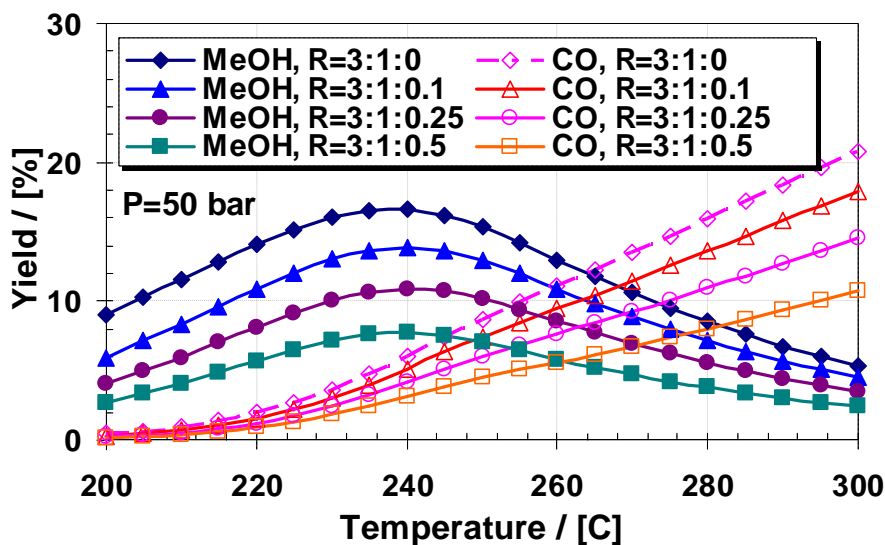


**Figure 6.** Effect of water presence (R=H<sub>2</sub>:CO<sub>2</sub>:H<sub>2</sub>O) on the MeOH and CO yield, at fixed pressure and along a temperature range (simulated results)

1  
2  
3  
4  
5  
6  
7  
8  
9  
10  
11  
12

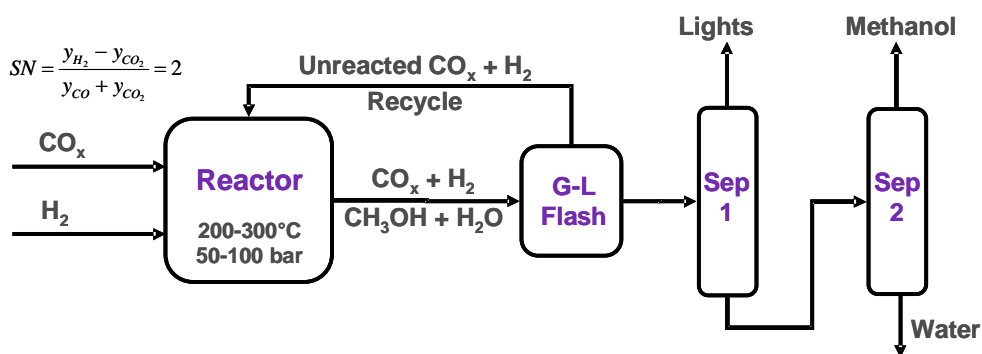


**Figure 7.** Generic processing scheme for methanol synthesis from syngas or by CO<sub>2</sub> hydrogenation

13  
14  
15  
16

